

REPORT DOCUMENTATION PAGE			Form Approved OMB NO. 0704-0188		
<p>The public reporting burden for this collection of information is estimated to average 1 hour per response, including the time for reviewing instructions, searching existing data sources, gathering and maintaining the data needed, and completing and reviewing the collection of information. Send comments regarding this burden estimate or any other aspect of this collection of information, including suggestions for reducing this burden, to Washington Headquarters Services, Directorate for Information Operations and Reports, 1215 Jefferson Davis Highway, Suite 1204, Arlington VA, 22202-4302. Respondents should be aware that notwithstanding any other provision of law, no person shall be subject to any penalty for failing to comply with a collection of information if it does not display a currently valid OMB control number. PLEASE DO NOT RETURN YOUR FORM TO THE ABOVE ADDRESS.</p>					
1. REPORT DATE (DD-MM-YYYY) 07-01-2008		2. REPORT TYPE Final Report		3. DATES COVERED (From - To) 18-Aug-2003 - 17-Aug-2007	
4. TITLE AND SUBTITLE Nanometer-Size Magnetic Devices			5a. CONTRACT NUMBER DAAD19-03-1-0298		
			5b. GRANT NUMBER		
			5c. PROGRAM ELEMENT NUMBER 611102		
6. AUTHORS Sy-Hwang Liou			5d. PROJECT NUMBER		
			5e. TASK NUMBER		
			5f. WORK UNIT NUMBER		
7. PERFORMING ORGANIZATION NAMES AND ADDRESSES University of Nebraska Research Grants & Contracts 303 Administration Bldg. Lincoln, NE 68588 -0430			8. PERFORMING ORGANIZATION REPORT NUMBER		
9. SPONSORING/MONITORING AGENCY NAME(S) AND ADDRESS(ES) U.S. Army Research Office P.O. Box 12211 Research Triangle Park, NC 27709-2211			10. SPONSOR/MONITOR'S ACRONYM(S) ARO		
			11. SPONSOR/MONITOR'S REPORT NUMBER(S) 45073-MS-DPS.16		
12. DISTRIBUTION AVAILABILITY STATEMENT Approved for Public Release; Distribution Unlimited					
13. SUPPLEMENTARY NOTES The views, opinions and/or findings contained in this report are those of the author(s) and should not be construed as an official Department of the Army position, policy or decision, unless so designated by other documentation.					
14. ABSTRACT This research is to understand the relationship between the local magnetic domain changes and the magnetization reversal behaviors of nanometer-sized magnetic features and to develop improved methods for understanding and characterizing the magnetic properties of nanometer-sized materials. We have developed a few advanced cantilevers for magnetic characterization of small magnetic objects. We have studied magnetic layers in magnetic sensors.					
15. SUBJECT TERMS Magnetic domain structure; Magnetic force microscopy tips; Magnetic patterned films, Magnetic sensors					
16. SECURITY CLASSIFICATION OF:		17. LIMITATION OF ABSTRACT		15. NUMBER OF PAGES	19a. NAME OF RESPONSIBLE PERSON
a. REPORT U	b. ABSTRACT U	c. THIS PAGE U	SAR		Sy Liou
					19b. TELEPHONE NUMBER 402-472-2405

Report Title

Nanometer-Size Magnetic Devices

ABSTRACT

This research is to understand the relationship between the local magnetic domain changes and the magnetization reversal behaviors of nanometer-sized magnetic features and to develop improved methods for understanding and characterizing the magnetic properties of nanometer-sized materials. We have developed a few advanced cantilevers for magnetic characterization of small magnetic objects. We have studied magnetic layers in magnetic sensors.

List of papers submitted or published that acknowledge ARO support during this reporting period. List the papers, including journal references, in the following categories:

(a) Papers published in peer-reviewed journals (N/A for none)

1. L. Gao, L. Yue, T. Yokota, R. Skomski, S. H. Liou, H. Takahoshi, H. Saito, and S. Ishio, "Focused Ion Beam Milled CoPt Magnetic Force Microscopy Tips for High Resolution Domain Images", IEEE Trans. on Magnetics, 40, 2194 (2004).
2. T. Yokota, L. Gao, S. H. Liou, M. L. Yan and D. J. Sellmyer, "Effect of Au Spacer Layer on L10 Phase Ordering Temperature of CoPt Thin Films", J. Appl. Phys., 95, 7270 (2004).
3. L. Gao, D. Q. Feng, L. Yuan, T. Yokota, R. Sabirianov, S. H. Liou, M. D. Chabot, D. Porpora, and J. Moreland, "A Study of Magnetic Interactions of Ni₈₀Fe₂₀ Arrays using Ultra-Sensitive Microcantilever Torque Magnetometry", J. Appl. Phys., 95, 7010 (2004).
4. M. L. Yan, R. Skomski, A. Kashyap, L. Gao, S. H. Liou and D. J. Sellmyer, "Hysteresis of Granular FePt:Ag Films with Perpendicular Anisotropy", IEEE Trans. on Magnetics, 40, 2495 (2004).
5. K. D. Sorge, A. Kashyap, R. Skomski, L. Yue, L. Gao, R. D. Kirby, S. H. Liou, and D. J. Sellmyer, "Interactions and Switching Behavior of Anisotropy Magnetic Dots", J. Appl. Phys., 95, 7414 (2004).
6. S. H. Liou, "Advanced Magnetic Force Microscopy Tips for Imaging Domains" Review Chapters in Nanostructured Advanced Magnetic Materials, eds. Y. Liu, D.J. Sellmyer, D. Shindo, Kluwer Academic Publishers 130-153 (2004)
7. T. Yokota, L. Gao, R. Zhang, L. Nicholl, M. Yan, D. J. Sellmyer, S. H. Liou, "The Perpendicular Magnetic Anisotropy of CoPt/Au Multilayer Films", J. of Magnetism and Magnetic Materials, 286, 301 (2005).
8. T. Yokota, M. Yan, Y. Xu, L. Gao, R. Zhang, L. Nicholl, L. Yuan, R. Skomski, D. J. Sellmyer, S. H. Liou, C. Lai, and C. Yang, "Magnetic Properties and L10 Phase Formation of FePt Films Prepared by High Current-Density Ion-Beam Irradiation and Rapid-Thermal Annealing Methods", J. Appl. Phys., 97, 10H306 (2005).
9. L. Yuan, J. X. Shen, Bharat B. Pant, and S. H. Liou, "Imaging magnetic noise sources in magnetic recording heads (invited)" SPIE 5843 (2005)
10. Michelle D. Chabot, John M. Moreland, Lan Gao, Sy-Hwang Liou, and Casey W. Miller, "Novel Fabrication of Micromechanical Oscillators with Nanoscale Sensitivity at Room Temperature", the Journal of MicroElectroMechanical Systems (MEMS), 14, 1118 (2005).
11. L. Yuan, S. H. Liou and Dexin Wang, "Temperature Dependence of Magnetoresistance in Magnetic Tunneling Junctions with different free layer structures", Phys. Rev. B, 73, 134403 (2006).
12. A. Baruth, D.J. Keavney*, J.D. Burton, K. Janicka, E.Y. Tsybal, L. Yuan, S.H. Liou, S. Adenwalla, "Origin of the interlayer exchange coupling in [Co/Pt]/NiO/[Co/Pt] multilayers studied with XAS, XMCD, and micromagnetic modeling", Phys. Rev. B, 74, 054419 (2006).
13. J. Shi, Y. F. Lu, K. J. Yi, Y. S. Lin and S. H. Liou, J. B. Hou and X. W. Wang "Direct synthesis of single-walled carbon nanotubes bridging metal electrodes by laser-assisted chemical vapor deposition", Appl. Phys. Lett., 89, 083105 (2006)
14. Aliakber Aktag, Steven Michalski, Lanping Yue, Roger D. Kirby, and Sy-Hwang Liou, "Formation of an Anisotropy Lattice in Co/Pt Multilayers by Direct Laser Interference Patterning", J. Appl. Phys., 99, 093901 (2006).
15. L. Yuan, L. Gao, R. Sabirianov, S. H. Liou, M. D. Chabot, D. H. Min, J. Moreland and Bao Shan Han, "Microcantilever Torque Magnetometry Study of Patterned Magnetic Film", IEEE Trans. on Magnetics, 42, 3234 (2006).
16. Brett Barwich, Glen Gronniger, Lu, Yuan, Sy-Hwang Liou, and Herman Batelaan, "A measurement of electron-wall interactions using transmission diffraction from nano-fabricated gratings", J. Appl. Phys., 100, 074322 (2006).
17. A. Baruth, L. Yuan, J.D. Burton, K. Janicka, E.Y. Tsybal, S.H. Liou, S. Adenwalla, "Domain overlap in exchange-coupled [Co/Pt]/NiO/[Co/Pt] multilayers" Appl. Phys. Lett., 89, 202505 (2006)
18. Chih-Huang Lai, Sheng-Huang Huang, C. C. Chiang, S. H. Liou, D. J. Sellmyer M. L. Yan, L. Yuan and T. Yokota, "Effects of ion-beam irradiation on the L10 phase transformation and their magnetic properties of FePt and PtMn films" (invited) Mater. Res. Soc. Symp. Proc. 887, 0887-Q07-05, 183-194 (2006).
19. L. Yuan, Y. S. Lin, Dexin Wang and S. H. Liou, "Tuning Magnetic Microstructure of Reference Layer in Magnetic Tunneling Junctions", IEEE Trans. on Magnetics, 43, 2788(2007).

Number of Papers published in peer-reviewed journals: 19.00

(b) Papers published in non-peer-reviewed journals or in conference proceedings (N/A for none)

(c) Presentations

1. L. Gao, L. Yue, T. Yokota, R. Skomski, S. H. Liou, H. Takahoshi, H. Saito, and S. Ishio, "Focused ion beam milled CoPt magnetic force microscopy tips for high resolution domain images", Presented at 9th Joint MMM-Intermag Conference, Anaheim, California, January 5-9, 2004.
2. T. Yokota, L. Gao, S. H. Liou, M. L. Yan and D. J. Sellmyer, "Magnetic properties of ultra-thin CoPt films with Au layer inserted", Presented at 9th Joint MMM-Intermag Conference, Anaheim, California, January 5-9, 2004.
3. L. Gao, D. Q. Feng, L. Yuan, T. Yokota, R. Sabirianov, and S. H. Liou, "A study of magnetic interactions of Ni₈₀Fe₂₀ arrays using ultra-sensitive microcantilever torque magnetometry", Presented at 9th Joint MMM-Intermag Conference, Anaheim, California, January 5-9, 2004.
4. D. J. Sellmyer, M. L. Yan, R. Skomski, A. Kashyap, L. Gao, and S. H. Liou, "Hysteresis of Granular FePt:Ag Films with Perpendicular Anisotropy", Presented at 9th Joint MMM-Intermag Conference, Anaheim, California, January 5-9, 2004.
5. K. D. Sorge, A. Kashyap, R. Skomski, L. Yue, L. Gao, R. D. Kirby, S. H. Liou, and D. J. Sellmyer, "Interactions and Switching behavior Behavior of Anisotropy Magnetic Dots", Presented at 9th Joint MMM-Intermag Conference, Anaheim, California, January 5-9, 2004.
6. L. Gao, D. Q. Feng, L. Yuan, T. Yokota, S. H. Liou, M. D. Chabot, and J. Moreland, "A study of the magnetic hysteresis of a single patterned magnetic element using a microcantilever torque magnetometer" Bull. of American Physical Society, Vol. 49, (2004).
7. T. Yokota, M. Yan, Y. Xu, L. Gao, R. Zhang, L. Nicholl, L. Yuan, R. Skomski, D. J. Sellmyer, S. H. Liou, "The perpendicular magnetic anisotropy of CoPt/Au multilayer films", J. of Magnetism and Magnetic Materials, (2004-5).
8. T. Yokota, M. Yan, Y. Xu, L. Gao, R. Zhang, L. Nicholl, L. Yuan, R. Skomski, D. J. Sellmyer, S. H. Liou, C. Lai, and C. Yang, "Magnetic Properties and L10 Phase formation of FePt films prepared by high current-density ion-beam irradiation and rapid-thermal annealing methods", Presented at 49th Annual Conference on Magnetism and Magnetic Materials, Jacksonville, Florida, November 7-11, 2004.
9. M. D. Chabot, J. Moreland, L. Gao, S. H. Liou and Casey W. Miller, "Ultra-Sensitive Micromechanical Cantilevers with Integrated Magnetic Structures" Bull. of American Physical Society, Vol. 50, 1131(2005).
10. Lan Gao, L. Yuan, K. H. P. Kim, S. H. Liou, M. D. Chabot, D. H. Min, and J. Moreland, "A study of the Magnetic Hysteresis of a Single Magnetic Elements using a Sensitive Microcantilever magnetometer" Bull. of American Physical Society, Vol. 50, 1492(2005).
11. A. Baruth, S.H. Liou, S. Adenwalla, and D.J. Keavney, "Effects of coupling on domain structure of [Pt(6°A)/Co(4°A)]₃/NiO(tNiO)/[Co(4°A)/Pt(6°A)]₃ multilayers with oscillatory coupling" Bull. of American Physical Society, Vol.51, (2006).
12. L Yuan, L. Gao, L. Nicholl, S. H. Liou, M. Zheng, E. N. Abarra, B. A. Acharya, G. Choe and Bao Shan Han, "Magnetic Force Microscopy Study of CoPtCrO Perpendicular Media with Superparamagnetic and Permanent Tips", Presented at IEEE International Magnetism Conference, San Diego California, May 8-12, 2006.
13. L. Yuan, L. Gao, R. Sabirianov, S. H. Liou, M. D. Chabot, D. H. Min, J. Moreland and Bao Shan Han, "Microcantilever Torque Magnetometry Study of Patterned Magnetic Film", Presented at IEEE International Magnetism Conference, San Diego California, May 8-12, 2006.
14. L. Yuan, Y. S. Lin, Dexin Wang and S. H. Liou, "Tuning Magnetic Microstructure of Reference Layer in Magnetic Tunnel Junctions", Presented at 10th Joint MMM-Intermag Conference, Baltimore, Maryland, January 7-11, 2007.
15. A. Baruth, L. Yuan, J. D. Burton, K. Janicka, E.Y. Tsymal, S.H. Liou, and S. Adenwalla, "Domain overlap in antiferromagnetically coupled [Co/Pt]/NiO/[Co/Pt] multilayers" Bull. of American Physical Society, Vol. 52, (2007).
16. John Moreland, Jason Eckstein, Yushun Lin, Sy-Hwang Liou, Steven Ruggiero, "Magnetic particle imaging with a cantilever torque magnetometer" Bull. of American Physical Society, Vol. 52, (2007).
17. S. H. Liou, Rui Zhang, L. Yuan, David P. Pappas and Bao Shan Han, "L10 phase FePt magnetic force microscopy probes for magnetic domain images", present at AVS 4th International Symposium & Exhibition, October 14-19, 2007 Washington State Convention Center, Seattle, Washington, USA.
18. S. H. Liou, Rui Zhang, Stephen E. Russek, L. Yuan, Sean T. Halloran, and David P. Pappas, "Dependence of noise in magnetic tunnel junction sensors on annealing field and temperature" Presented at 52nd Annual Conference on Magnetism and Magnetic Materials, Tampa, Florida, November 5-9, 2007.
19. A. Baruth, L. Yuan, J. D. Burton, K. Janicka, E.Y. Tsymal, S.H. Liou, and S. Adenwalla, "Domain overlap in antiferromagnetically coupled [Co/Pt]/NiO/[Co/Pt] multilayers", Presented at 52nd Annual Conference on Magnetism and Magnetic Materials, Tampa, Florida, November 5-9, 2007.
20. S. H. Liou, Rui Zhang, Stephen E. Russek, L. Yuan, Sean T. Halloran, and David P. Pappas "Noise study of magnetic tunnel junction sensors with magnetic flux concentrators", Partners in Environmental Technology Technical Symposium & Workshop December 4-6, 2007, at the Marriott Wardman Park Hotel in Washington, D.C.

Number of Presentations: 20.00

Non Peer-Reviewed Conference Proceeding publications (other than abstracts):

Number of Non Peer-Reviewed Conference Proceeding publications (other than abstracts):

0

Peer-Reviewed Conference Proceeding publications (other than abstracts):

Number of Peer-Reviewed Conference Proceeding publications (other than abstracts):

0

(d) Manuscripts

20. S. H. Liou, Rui Zhang, Stephen E. Russek, L. Yuan, Sean T. Halloran, and David P. Pappas, "Dependence of noise in magnetic tunnel junction sensors on annealing field and temperature" accepted J. Appl. Phys., (2008)

21. I.-C. Chen, L.-H. Chen, A. I. Gapin, S. Jin, L. Yuan and S.-H. Liou, "Iron-platinum coated carbon nanocone probes on tipless cantilevers for high resolution magnetic force imaging", Nanotechnology (Submitted) (2008).

Number of Manuscripts: 2.00

Number of Inventions:

Graduate Students

<u>NAME</u>	<u>PERCENT SUPPORTED</u>
Lan Gao	0.25
Lu Yuan	0.25
Danqin Feng	0.10
LeighAnn Nicholl	0.10
Rui Zhang	0.10
Yushun Lin	0.10
FTE Equivalent:	0.90
Total Number:	6

Names of Post Doctorates

<u>NAME</u>	<u>PERCENT SUPPORTED</u>
FTE Equivalent:	
Total Number:	

Names of Faculty Supported

<u>NAME</u>	<u>PERCENT SUPPORTED</u>	National Academy Member
Sy-Hwang Liou	0.25	No
Renat Sabirianov	0.10	No
FTE Equivalent:	0.35	
Total Number:	2	

Names of Under Graduate students supported

<u>NAME</u>	<u>PERCENT SUPPORTED</u>
Wenjin Zhou	0.10
FTE Equivalent:	0.10
Total Number:	1

Student Metrics

This section only applies to graduating undergraduates supported by this agreement in this reporting period

- The number of undergraduates funded by this agreement who graduated during this period: 1.00
- The number of undergraduates funded by this agreement who graduated during this period with a degree in science, mathematics, engineering, or technology fields:..... 1.00
- The number of undergraduates funded by your agreement who graduated during this period and will continue to pursue a graduate or Ph.D. degree in science, mathematics, engineering, or technology fields:..... 1.00
- Number of graduating undergraduates who achieved a 3.5 GPA to 4.0 (4.0 max scale):..... 1.00
- Number of graduating undergraduates funded by a DoD funded Center of Excellence grant for Education, Research and Engineering:..... 0.00
- The number of undergraduates funded by your agreement who graduated during this period and intend to work for the Department of Defense 0.00
- The number of undergraduates funded by your agreement who graduated during this period and will receive scholarships or fellowships for further studies in science, mathematics, engineering or technology fields: 1.00

Names of Personnel receiving masters degrees

<u>NAME</u> Rui Zhang Danqin Feng Yushun Lin Total Number:	 3
---	--------------------------

Names of personnel receiving PHDs

<u>NAME</u> Lan Gao Lu Yuan Total Number:	 2
---	----------------------

Names of other research staff

<u>NAME</u>	<u>PERCENT SUPPORTED</u>
FTE Equivalent:	
Total Number:	

Sub Contractors (DD882)

Inventions (DD882)

The problem studied:

This research is to understand the relationship between the local magnetic domain changes and the magnetization reversal behaviors of nanometer-sized magnetic features and to develop improved methods for understanding and characterizing the magnetic properties of nanometer-sized materials. We have developed a few advanced cantilevers for magnetic characterization of small magnetic objects. We have studied magnetic layers in magnetic sensors.

A few examples as follows:

- (1) Magnetic properties of ultra-thin CoPt films with Au layer inserted
- (2) Magnetic Force Microscopy Study of CoPtCrO Perpendicular Media With Superparamagnetic And Permanent Magnet Tips
- (3) Focused Ion Beam Milled CoPt Magnetic Force Microscopy Tips for High Resolution Domain Images
- (4) Batch Fabricated High-resolution MFM Tips for Both Soft and Hard Magnetic Materials
- (5) Microcantilever Torque Magnetometry Study of Patterned Magnetic Films
- (6) Torsion Oscillator Magnetic Field Sensors
- (7) Imaging Magnetic Noise Sources in Magnetic Recording Heads
- (8) Dependence of Noise in Magnetic Tunnel Junction Sensors on Annealing Field and Temperature

Summary of the most important results:

(1) Magnetic properties of ultra-thin CoPt films with Au layer inserted

We investigated the reduction in the ordering temperature using a CoPt multilayer with Au layer inserted. It was revealed that the adding of Au is effective for reducing the ordering temperature by about 200 °C. From the structural analysis, the phase formation of the L1₀ structure of the Au inserted CoPt layer films starts at around 350 ~ 400 °C. At the same temperature, the H_c of these films has drastic changes. It shows clearly that the occurrence of high H_c is related to the phase formation of L1₀ structure of CoPt. The study of the time dependence of H_c reveals that the phase formation of L1₀ structure of CoPt is a slow diffusion process.

Fig. 1 shows H_c at 300 K versus the annealing temperature (T_a) for the CoPt film with or without Au layer inserted. For as-deposited CoPt films, both with and without Au layers, the H_c at 300 K is about 30 Oe and the M-H curves exhibit soft magnetic properties. After annealing, the H_c of pure CoPt film changed slowly. The H_c of the pure CoPt film annealed at 550 °C is about 2 kOe. The H_c of the CoPt (3 nm)/Au (2 nm) multilayer films began to change at 350 °C and drastically increase over 400 °C. The H_c of the CoPt (3 nm)/Au (2 nm) multilayer sample annealed at 350 °C is about the same as that of pure CoPt films annealed at 550 °C. These results indicated clearly the effect of adding Au for the reduction of the processing temperature. Such a remarkable improvement of processing temperature due to the addition of Au can be better understood by the temperature dependence of structure changes. Fig. 2 shows the change in the d-spacing (d₁₁₁) versus T_a. The d-spacing of the CoPt (3 nm)/Au (2 nm) multilayer samples is rapidly decreased around 400 °C. The change in the lattice parameter has the same tendency as that of the H_c. Judging from these results, the phase formation of the L1₀ structure of the CoPt inserted Au layer films starts around 350 ~ 400 °C. And, in the sample with a 2 nm Au layer, a temperature of 400 °C is enough for a high coercivity (above 5 kOe).

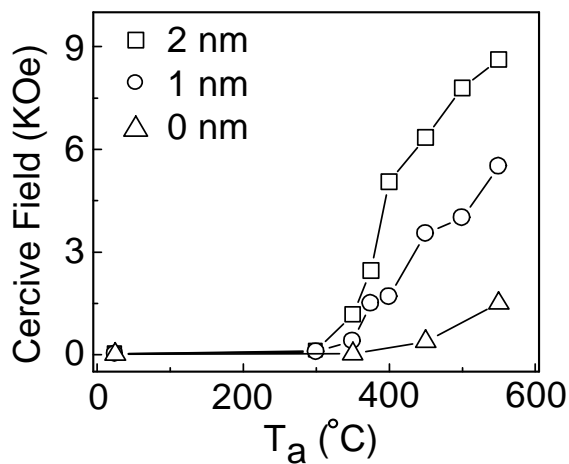


Fig. 1 Annealing temperature (T_a) dependence of the in-plane coercive force (H_c) for the different Au layer thickness. (Square is 2nm, open circle is 1 nm, and triangle is 0 nm, respectively.) The annealing time is 5 hours.

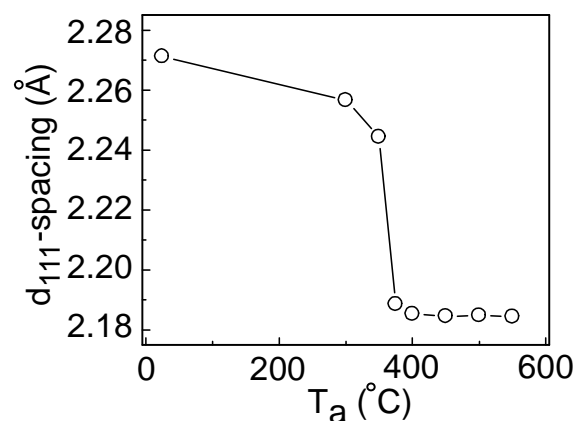


Fig. 2 Change in the d-spacing (d₁₁₁) versus the annealing temperature (T_a) of the film with 2 nm Au layer with various annealing temperatures (25 – 550 °C).

(2) Magnetic Force Microscopy Study of CoPtCrO Perpendicular Media With Superparamagnetic And Permanent Magnet Tips

Magnetic force microscopy (MFM) has been widely used in the study of magnetic recording media. It requires high resolution MFM tips as well as better understanding of the obtained magnetic images. In this study, we compared the images obtained by superparamagnetic and permanent magnet MFM tips, which allowed us to explain the issues related to the frequency doubling in some domain images of the recording media. As shown in Fig. 3, we compared the magnetic (phase) image of the 200 kfc/i track in an ac-erased area taken with a permanent magnet and a superparamagnetic tip. Fig. 3a is the image obtained by the permanent magnet MFM tip, which shows a dominant spectral frequency of about 200 kfc/i. Fig. 3b is the image taken by a superparamagnetic tip, which shows a dominant spectral frequency of about 400 kfc/i. The frequency doubling was clearly observed by using a superparamagnetic tip. This may explain the observation of frequency doubling by Zhifeng Deng et al. in their phase images of a PMR medium using metal-coated carbon nanotube tips. We show that the magnetic images obtained by different types of MFM tips can provide valuable magnetic information about the sample.

In summary, to study magnetic images, using more than one type of tip may help in the quantitative analysis of MFM data.

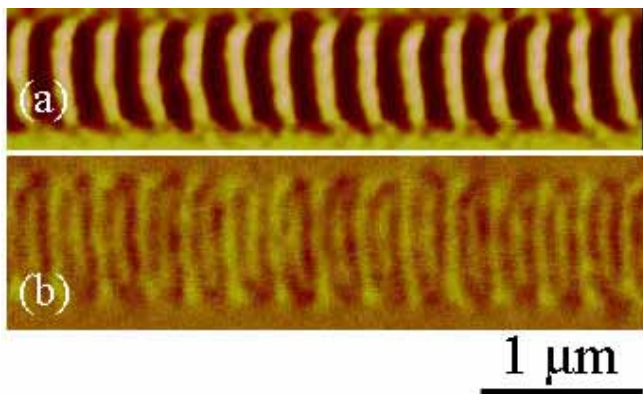


Fig. 3 Magnetic (phase) images of the 200 kfc/i track in an ac-erased area taken with (a) a permanent magnetic tip and (b) a superparamagnetic tip.

(3) Focused Ion Beam Milled CoPt Magnetic Force Microscopy Tips for High Resolution Domain Images

High coercivity CoPt magnetic force microscope tips have been modified by focused ion beam milling to improve the resolution of magnetic domain images. The magnetic materials around the apex have been removed leaving a 30 nm diameter magnetic particle at the tip end (as shown in Fig. 4). Due to the smaller amount of magnetic material, the stray field from this new tip is significantly reduced and the spatial resolution of magnetic domain images is improved. The tip is used to obtain high resolution domain images of a CoCrPt-SiO₂/Ru perpendicular recording medium with linear recording densities from 800 to 1000 kfc/i. Magnetic patterns of 900 kfc/i, corresponding to a bit size of 28 nm, are well resolved. From the analysis of the power spectrum of the track profiles for these images, a spatial resolution as good as 11 nm under ambient conditions with a commercial magnetic force microscope is achieved.

The resolution of the MFM can be characterized in real space by its “point response” or in Fourier transform space by its wave-vector (spatial frequency) response. Essentially, the two approaches are equivalent. Fig. 5 shows the domain images of recording tracks with linear recording densities from 800 to 1000 kfc/i (kilo flux changes per inch). Tracks of 800, 900 and

1000 kfcI correspond to bit sizes of 32, 28 and 25 nm, respectively. The MFM image of the 800 kfcI track presents well-resolved recording bits. Track densities up to 900 kfcI are clearly visible by MFM. The visibility of the 1000 kfcI track transitions is much less pronounced.

Fig. 6(a) shows the power spectrum of the 800 kfcI track. The peak corresponds to the recorded signal with a wave length of 73 nm (which is double the recording bit size). This value is higher than the calculated value of 64 nm for 800 kfcI. This may be due to inaccuracies in the recording process. As shown in Fig. 6(c), the peak corresponds to the recorded signal of a 1000 kfcI track with a wavelength of 58 nm and is only resolved by Fourier transform. In Fig. 6(a), a wavelength cutoff of 22 nm is obtained from the intersection of the signal and the noise. This corresponds to an MFM image resolution of 11 nm, which is half the wavelength. For the 900 and 1000 kfcI tracks, the resolutions obtained from the wavelength cutoffs are 12 and 11 nm, respectively, as shown in Fig. 6(b) and 6(c). The error of the resolution is about 2 nm, which is due to the inaccuracies of drawing the signal line and the noise line.

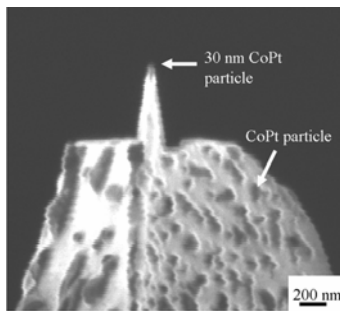


Fig. 4. An FIB milled MFM tip shows a magnetic particle with a diameter of 30 nm at the tip end.

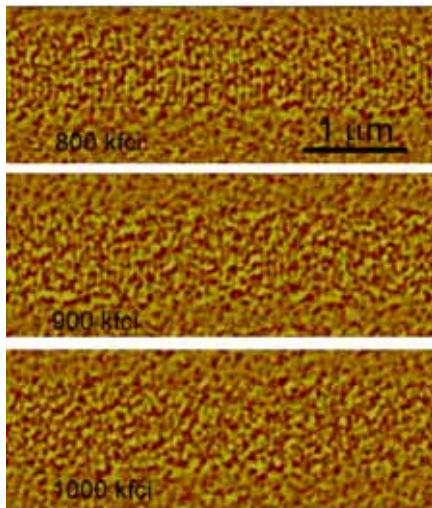


Fig. 5 Magnetic domain images of a recording disk with different writing bit density, 800 kfcI, 900 kfcI and 1000 kfcI.

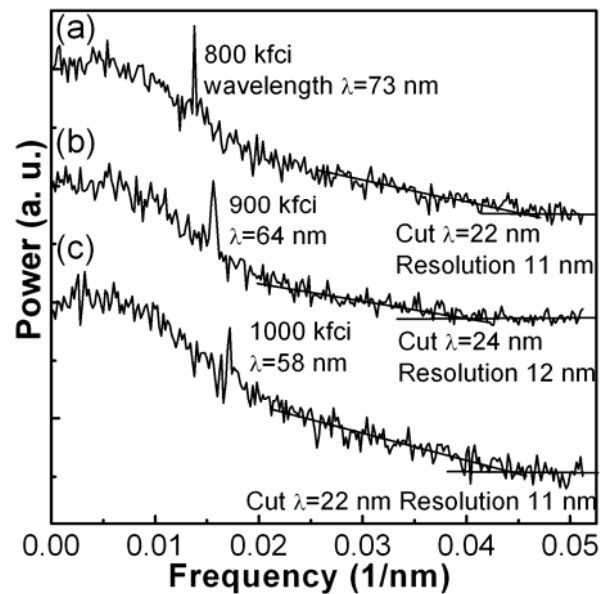


Fig. 6 An FFT analysis method is used to analyze the power spectrum of the profile by Fourier transformation. The resolution is (a) 11 nm for the 800 kfcI track, (b) 12 nm for 900 kfcI, and (c) 11 nm for 1000 kfcI.

(4) Batch Fabricated High-resolution MFM Tips for Both Soft and Hard Magnetic Materials

Magnetic force microscopy (MFM) is one of the most often used techniques in the investigation of surface magnetic structures. The MFM probe consists of a very sharp magnetic tip mounted on a soft cantilever. When the probe scans over the sample, the force acting on the tip due to the stray field emanating from the sample is detected. The resolution of the MFM images is determined by the tip's size and magnetic properties. An ideal MFM tip should have a small physical size for the magnetic material at the very end of the tip, which defines the minimum detectable magnetic feature size. To obtain detectable interaction between the small size tip and the sample with an adequate signal-to-noise ratio, a sufficient magnetization of the magnetic material at the end of tip is required. Materials with higher saturation magnetization, M_s , are preferred. Another important parameter is the coercivity (H_c) of the MFM tip. If it is lower than the magnetic stray field of the sample, the magnetization direction of a MFM tip will be changed or moved during measurement. As a result, the magnetic images are difficult to explain. The MFM detects the long-range interactions that include not only the interaction between the sample and the magnetic materials near the tip, but also from the extended area of the tip. This makes the MFM images more difficult to interpret and reduces the MFM image resolution. The stray field from the extended area can be reduced by modifying the tip shape or by developing tip coating techniques. In this work, we show batch-fabricated high-resolution FePt-coated MFM probes with high H_c , high M_s , and low stray field. We also present the MFM images of a garnet (soft) and a permanent magnet (hard) taken with the same tips.

The tips are made from commercial silicon micro-machined cantilevers with spring constants of 1-5 N/m, resonant frequencies of 70-89 kHz, and quality factors of about 200 in air. The thin FePt alloy films were made by dc magnetron sputtering. The film thickness was around 20 nm. These FePt MFM tips have a H_c of about 1 T and M_s of about 900 emu/cm³.

Fig. 7 (a) and Fig. 8 are the MFM images of a garnet and a permanent FeNdB magnet using the same MFM tip. Fig. 7(b) is the MFM image that uses a commercial MFM tip.

In summary, we showed that the batch fabricated FePt coated MFM tips can be used to scan both soft and hard magnetic samples.

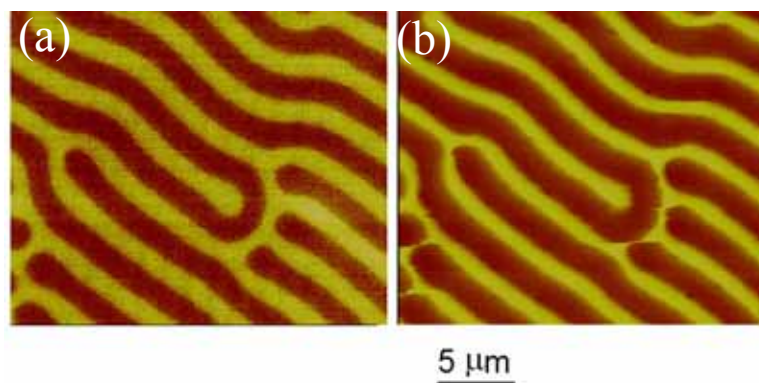


Fig. 7 MFM images of a garnet in the same area using (a) a new developed FePt MFM tip, (b) a commercial tip.

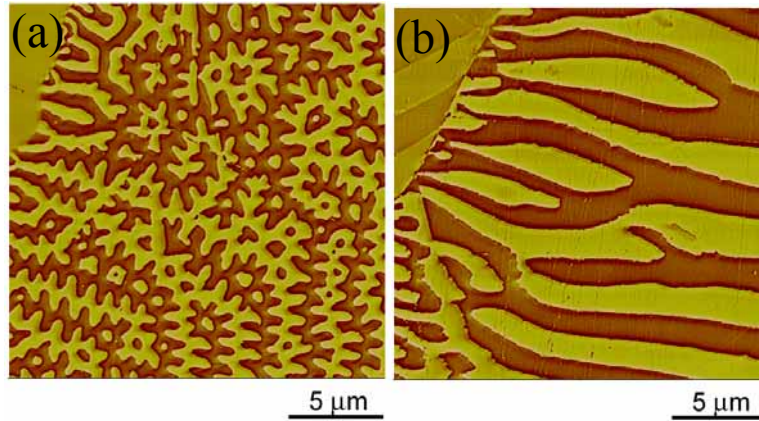


Fig. 8 MFM images of a permanent FeNdB magnet using a newly developed FePt MFM tip. (a) The domain pattern of the surface perpendicular to c-axis (b) The domain pattern of the surface parallel to the c-axis

(5) Microcantilever Torque Magnetometry Study of Patterned Magnetic Films

The study of small, defined magnetic structures has attracted much attention due to interest in both technological applications and fundamental research in micromagnetism. Microcantilever torque magnetometry (MTM) is a promising new experimental technique for measuring such small magnetic features. One of the challenges of using this technique is to place the sample on the cantilever. In this work, we develop a new process for preparing a patterned magnetic film on cantilever and show a primary result for magnetic interactions in a paired magnetic bar measured by MTM.

The process of patterning the magnetic film on the cantilever is the following: (a) deposit a multilayer Au (200 nm)/Cr (10 nm) on the cantilever, (b) patterning using focused ion beam (FIB) milling, (c) magnetic film deposition through a mask, and (d) a lift-off process. The magnetic hysteresis loops of the patterned dots arrays are measured by MTM at ambient conditions. Fig. 9 shows the measured hysteresis loop for a dot array with a dot diameter of 500 nm and center-to-center distance of 2 μm. The vortex state is formed at 26 kA/m, and the single domain state happens at -49 kA/m.

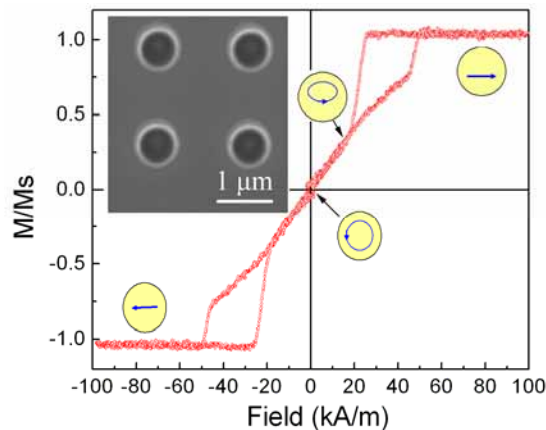


Fig. 9 A hysteresis loop for a 50 nm-thick Ni₈₀Fe₂₀ array of 100 dots with a diameter of 500 nm and center-to-center distance of 2 μm.

In order to understand the magnetic interaction between a pair of bars, we prepared a sample as shown in Fig. 10. A $7\ \mu\text{m} \times 7\ \mu\text{m} \times 30\ \text{nm}$ $\text{Ni}_{80}\text{Fe}_{20}$ film was put on the top left corner of the MTM cantilever. The $\text{Ni}_{80}\text{Fe}_{20}$ film was then patterned by a FIB workstation into two single $7\ \mu\text{m} \times 3.5\ \mu\text{m} \times 30\ \text{nm}$ bars by cutting a $50\ \text{nm}$ gap in the center of the film [Fig. 10(a)]. After the measurement, the top bar was removed with FIB milling and just left a single $7\ \mu\text{m} \times 3.5\ \mu\text{m} \times 30\ \text{nm}$ bar on the cantilever [Fig. 10(b)].

Magnetic properties of the patterned $\text{Ni}_{80}\text{Fe}_{20}$ films were characterized using a MTM at room temperature and in air. All measurements were done with a magnetic field applied in plane and perpendicular to the axis of the cantilever, as marked in the top of Fig. 10(a). Fig. 11 shows the magnetic hysteresis loops for the single and paired $7\ \mu\text{m} \times 3.5\ \mu\text{m} \times 30\ \text{nm}$ $\text{Ni}_{80}\text{Fe}_{20}$ bars. For the single bar, the magnetization reversal occurs around the coercivity field of $-1.23\ \text{kA/m}$. It is correlated to the domain wall propagating quickly through the bar. The smaller jump in magnetization at $-4\ \text{kA/m}$ may be caused by the annihilation of the small domain structure at the edge of the film. For paired bars, the magnetization reversal occurs at $-1.3\ \text{kA/m}$ and $-1.7\ \text{kA/m}$. The first jump at a field of $-1.3\ \text{kA/m}$ corresponds to the reversal of one of the paired bars. The second jump at a field of $-1.7\ \text{kA/m}$ corresponds to the reversal of the other one. The fact that the switching field of single bars is larger than the reversing field of only one of the paired bars and less than that of both paired bars indicates magnetostatic interaction exists between the closely paired bars and that is consistent with our micromagnetic simulations.

In summary, we develop a process to pattern a magnetic film on the MTM cantilever and by using MTM, we studied the magnetic interaction between the close small size and shaped-defined magnetic elements with high resolution.

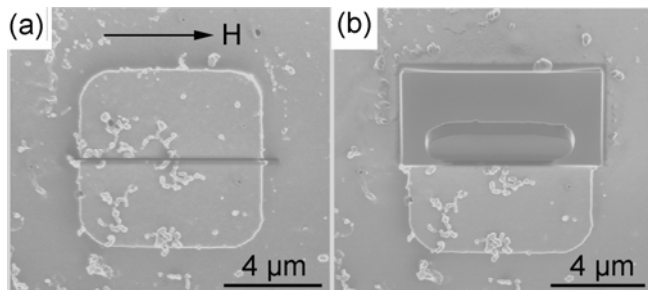


Fig. 10 (a) Double $7\ \mu\text{m} \times 3.5\ \mu\text{m} \times 30\ \text{nm}$ bars patterned with focused ion beam (FIB) on the $7\ \mu\text{m} \times 7\ \mu\text{m} \times 30\ \text{nm}$ $\text{Ni}_{80}\text{Fe}_{20}$ film with a gap of $50\ \text{nm}$ between adjacent bars. (b) Single $7\ \mu\text{m} \times 3.5\ \mu\text{m} \times 30\ \text{nm}$ bar after removing the top bar with FIB.

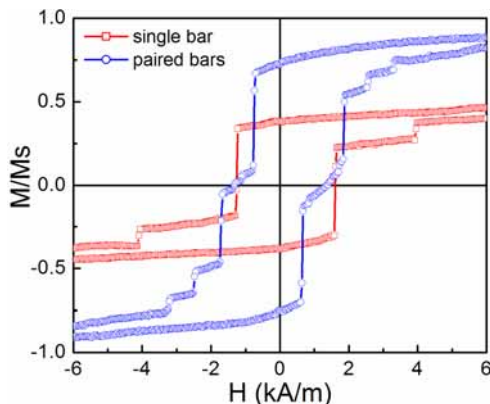


Fig. 11 Magnetic hysteresis loops obtained with a microcantilever torque magnetometer of the single $7\ \mu\text{m} \times 3.5\ \mu\text{m} \times 30\ \text{nm}$ $\text{Ni}_{80}\text{Fe}_{20}$ bar and same size paired bars with a gap of $50\ \text{nm}$.

(6) Torsion Oscillator Magnetic Field Sensors

Microcantilever torque magnetometry (MTM) is a promising new experimental technique for measuring such small magnetic features due to its high sensitivity. In this work, we develop a new sensitive magnetic sensor based on MTM that can detect nT range field change under ambient conditions and we expect pT sensitivity with further improvement.

The principle of the MTM sensor, $\tau = \vec{m} \times \vec{H}_t$, is shown in Fig. 12(a). τ is the torque that applied to the cantilever. The magnetic sample is magnetized (\vec{m}) by an applied magnetic field along the sample plane. A small ac torque magnetic field is applied perpendicular to the sample plane (\vec{H}_t) by a solenoid coil that excites the cantilever at the resonance frequency. Our current MTM can detect a magnetic moment change of 10^{-12} Am^2 with a $H_t = 10^{-4} \text{ T}$, that is, a change in $\tau = 10^{-16} \text{ N}\cdot\text{m}$ can be measured. As shown in Fig. 12(b), the lock-in signal is plotted as a function of time as the magnetic flux is stepped in 16 sec intervals. The mark shows that a 55 nT change in magnetic field has about 15 mV output from the lock-in amplifier.

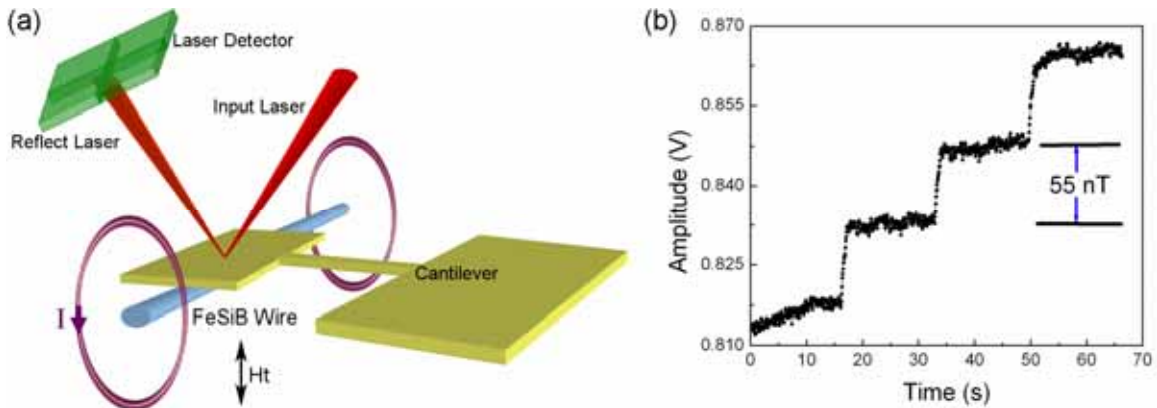


Fig. 12 (a) A schematic diagram of the set-up of the torsion oscillator magnetic field sensor, and (b) the lock-in signal is plotted as a function of time as the magnetic flux is stepped in 16 sec intervals. The mark is a 55 nT change in magnetic field.

(7) Imaging Magnetic Noise Sources in Magnetic Recording Heads

A detailed understanding of noise characteristics is essential for the design of a high signal-to-noise ratio (SNR) reader sensor. We intend to correlate the microstructure to the source of magnetic noises for improving the magnetic stability of the recording heads. A dynamic magnetic sensitivity mapping (MSM) system was designed to image the magnetic noise sources in sub-micrometer sized recording heads. A nanometer sized magnetic force microscopy (MFM) tip was used to apply a well-defined, localized magnetic field on the air bearing surface (ABS) of the head. For a certain area position of the free layer with incoherent rotation of the magnetic moment, this localized magnetic field will cause magnetic instability in the head, and this instability will show up as electrical noise in the output signal. Because most of the noise related to magnetic domain fluctuation is dominant in the low frequency region, our study concentrates on the spatial characterization of the noise source in a frequency range of 20 kHz to 60 kHz. Recording the average amplitude of the noise spectrum due to the excitation in the measured frequency range as a function of the tip's position, the location of the magnetic noise source can be identified. Magnetic noise images have been obtained by our system for some giant magnetoresistance (GMR) and tunneling magnetoresistance (TMR) recording heads. Noise MSM images of some unstable recording heads clearly show the spatially uneven noise

The noise mapping images of stable and unstable TMR heads with positive and negative tip magnetization in the frequency range of 20 kHz-60 kHz are shown in Fig. 13. For head I, the noise maps [Fig. 13(a) and (b)] show that there is no additional noise due to magnetic tip excitation whether under a positive or a negative tip magnetization state. However, the noise map for head 2 [Fig. 13(c)] shows that there is considerable noise having spatial variation. A magnetic noise increase is detected only during tip scanning over the left side of the sensor and a small amount of noise is observed in the right part of the sensor. Upon reversing the tip field direction, this localized magnetic noise disappears [Fig. 13(d)].

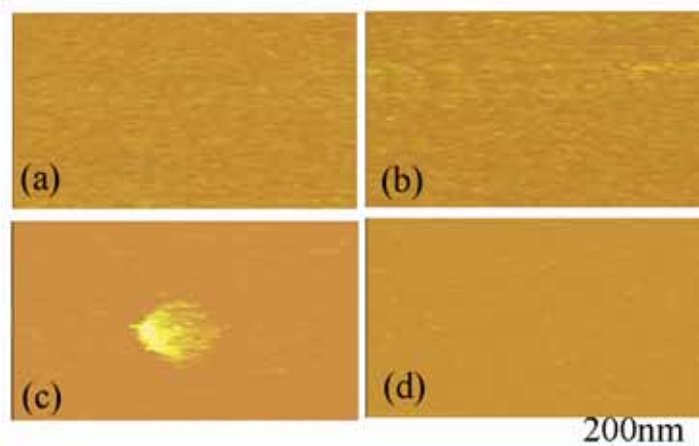


Fig. 13 MSM images for the TMR head I (stable) (a) under a positive magnetic field and (b) under a negative field; and for magnetic TMR head 2 (unstable) (c) under a positive magnetic field and (d) under a negative field.

(8) Dependence of Noise in Magnetic Tunnel Junction Sensors on Annealing Field and Temperature

Sensor noise is a crucial parameter in low-field applications and the minimum detectable field of the sensor is limited by their intrinsic noise. In order to resolve this issue, we investigated the low frequency noise in magnetic tunnel junctions (MTJs) which were configured into 64 element symmetric bridges as shown in Fig. 14. They were annealed in the temperature range from 265°C to 305°C and magnetic fields up to 7 T, either in helium or hydrogen environments. It can be seen from Fig. 15 that the noise level of the MTJ annealed in hydrogen gas at 0.5 T external magnetic field is reduced by two times at low frequency (at 1 Hz) compared with the original sample (which was annealed at 285°C and in 0.5 T field) and the noise level of the MTJ annealed under hydrogen gas at 7 T is reduced by three times at low frequency (at 1 Hz) compared with the original sample. The source of noise in MTJs can be magnetic or non-magnetic in origin, which can be distinguished by measuring in different magnetic fields. There is about an order of magnitude reduction of the low frequency noise spectrum when the MTJ is measured with a 10 mT bias magnetic field. (In this magnetic field the magnetization of the free layer is parallel to that of the pinned layer.) The reduction of the noise at low frequency might due to the removal of some of defects and the pinning sites change in the free layer as well as the pinning layer during the annealing in high magnetic field. By optimizing the annealing temperature in hydrogen, we may further improve the noise floor at low frequency in the future, in other words, improve the minimum detectable field of future sensors at low frequency.

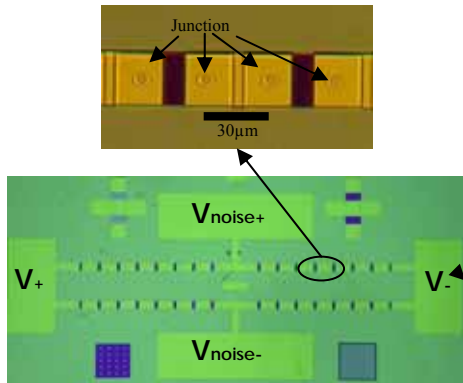


Fig. 14 The picture of the MTJ bridge with a junction size of 5 μm x 7.5 μm. Inset is an enlarged picture of those MTJs

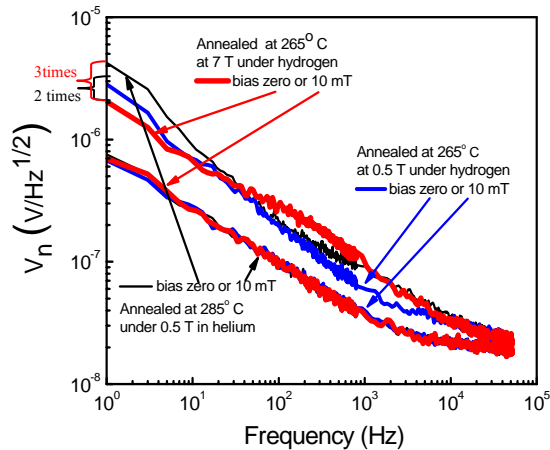


Fig.15 Noise spectrum of MTJ bridge with junction size 10 μm x 15 μm annealed at 265°C in fields of 0.5 T and 7 T in a hydrogen environment.